JOURNAL OF MATERIALS SCIENCE 30 (1995) 253–257

A high-resolution-electron-microscopy study of $\gamma/\gamma'-\alpha$ directionally solidified eutectic alloy

Part II *As-ageing treatment*

J. Y. DAI, D. X. LI, H. Q. YE, Z. X. JIN, J. H. ZHANG
Laboratory of Atomic Imaging of Solids, Institute of Metal Research, Chinese Academy of Sciences, Shenyang 110015, People's Republic of China

A master alloy with eutectic compositions of Ni–30.26Mo–6.08Al–1.43 V (wt%) has been directionally solidified (DS) into $\gamma/\gamma'-\alpha$ alloy. The microstructural as-ageing treatment was studied by means of high resolution electron microscopy (HREM). A majority of α fibres still display the Bain orientation relationship with the γ'/γ matrix. In a few cases, however, the so-called Nishiyama–Wasserman (NW) orientation relationship is found in specimens aged at 850 °C for 2000 h. Different microdomain structures of the γ phase, corresponding to different ageing temperatures, were revealed. Orthorhombic Ni_3Mo phase, with a size of tens of nanometres, was found to precipitate inside α fibres after ageing at both 850 and 650 °C. Occasionally, an γ'–Ni_3Al phase with lamellar twin structure was also found to coexist with Ni_3Mo precipitate inside the α fibres. The orientation relationships between the precipitates and the α fibres were determined. Energy dispersive X-ray analysis (EDX) showed that the precipitation of Ni_3Mo and Ni_3Al is due to solid solution of Ni and Al in the α fibres.

1. Introduction

Recently, there has been considerable attention paid to $\gamma/\gamma'-\alpha$ directionally solidified eutectic alloy for potential applications as advanced alloys for gas turbine blade components. These materials exhibit excellent mechanical properties at both high (900–1000 °C) and intermediate (600–850 °C) temperatures [1, 2]. Therefore, a study of the microstructure and character of the interface structure at high temperature is important, because the mechanical property, stability, can be expected to depend on these parameters [3].

Cellular Ni_3Mo, precipitated with orthorhombic Cu_3Ti structure, has been observed at grain boundaries in both Ni–12Al–15Mo and Ni–12.8Al–22.2Mo, heated at intermediate temperatures (600–850 °C) [4]. The occurrence of the cellular transformation may be considered as: $\gamma' + \gamma + Ni_xMo$ metastable precipitates $\rightarrow \gamma + Ni_3Mo$. In practice, the transformation was accompanied by a substantial loss in ductility [5].

Much work on phase transformation and on the morphology of α fibres during latter heat treatment has been done [6–8]. However, only a few papers have reported HREM studies of the structural transformation during heat treatment.

In this paper, phase transformation in the γ phase, due to the different phase transformation mechanisms at different temperatures, will be discussed. Fine precipitates of orthorhombic Ni_3Mo and γ'–Ni_3Al inside α fibres will also be revealed.

2. Experimental procedure

The $\gamma/\gamma'-\alpha$ alloy, with a nominal composition of Ni–30.26Mo–6.08Al–1.43 V (wt %), was directionally solidified in a DS furnace with a growth rate of 1.5 cm h^{-1}. The alloy was aged at 850 °C for 500 and 2000 h, and at 650 °C for 150 h in vacuum followed by water quenching. HREM samples were prepared by a conventional procedure which involved cutting discs with a diameter of 3.0 mm, mechanically polishing them to 50 μm thin, dimpling to 20 μm, and finally ion milling. HREM observations were performed in a Jem 2000EX II high resolution electron microscope with a point-to-point resolution of 0.21 nm. The EDX analysis was performed in a Philips EM 420 analytical electron microscope with a probe size of 50 nm.

3. Results and discussion

3.1. Morphology and orientation relationship after ageing

After long term ageing treatment at 850 and 650 °C, the typical morphology of α fibres is still rectangular in cross-section, delimitated by $\{1\,1\,0\}_\alpha$ facets within the γ'/γ matrix. This suggests that α fibres are relatively stable during long term ageing treatment. It can be expected that the relative stability of the α fibres, as a ductile strengthening phase, is possibly beneficial to the stability of the mechanical properties at high temperature.

Most α fibres still display the Bain orientation relationship with γ'/γ matrix, after ageing at both 850 and 650 °C. In a few cases, however, the so-called NW orientation relationship between the α fibre and $\gamma' - \gamma'$ phase was found in the specimen aged at 850 °C for 2000 h, i.e. $[0\,0\,1]_\alpha // [1\,\bar{1}\,0]_{\gamma'}$ and $(1\,1\,0)_\alpha \| (1\,1\,1)_{\gamma'}$. Fig. 1 shows the composite selected area electron

0022–2461

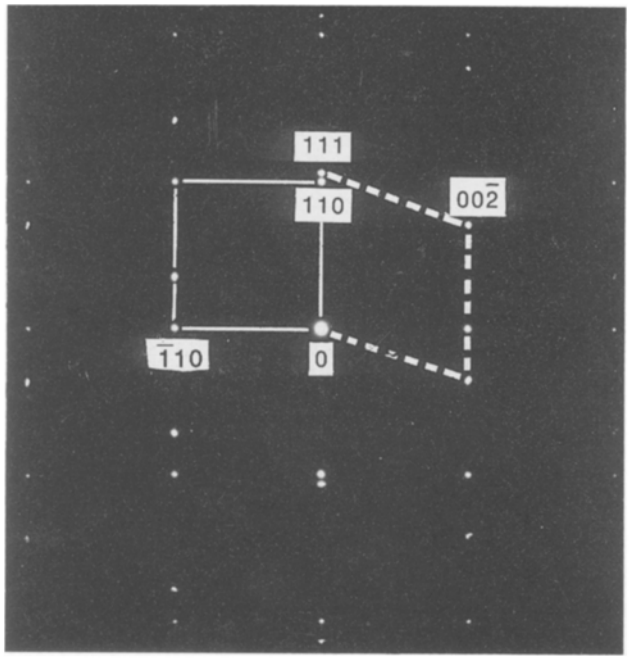

Figure 1 Composite electron diffraction patterns of the α fibre and γ′ phases, showing the NW orientation relationship.

diffraction (SAED), pattern of α and γ′ phases. At very thin regions of the specimen, the superlattice diffraction points of $\{0\,0\,1\}_{\gamma'}$ are too weak to appear in the diffraction pattern in Fig. 1.

3.2. HREM image of α/γ′ interface with NW orientation relationship

Fig. 2a is a transmission electron microscope (TEM) micrograph of the α/γ′ interface for the NW orientation relationship, showing four steps regularly arranged, with spacings ranging from 30 to 35 nm. The HREM image showing the fine structure of the interface step is presented in Fig. 2b. The interface is indicated by double arrows. An extra atomic plane of $(1\,1\,1)_{\gamma'}$ due to lattice mismatch between $(1\,1\,0)_{\alpha}$ and $(1\,1\,1)_{\gamma'}$ is indicated by the symbol "⊢". The lattice mismatch between $d_1 = d^{\alpha}_{(\bar{1}\,1\,0)}$ and $d_2 = d^{\alpha}_{(\bar{1}\,\bar{1}\,1)}\csc 70.5°$ [the $(\bar{1}\,\bar{1}\,1)_{\gamma'}$ closest-packed plane is inclined to the interface at an angle of 70.5°] at $(1\,1\,0)_{\alpha}\|(1\,1\,1)_{\gamma'}$ interface is about $\delta = 0.8\%$, and the mean spacing between misfit dislocations calculated by $Sd = |\vec{b}|/\delta$ is about 28 nm (where $\vec{b} = 1/2\langle\bar{1}\,1\,0\rangle_{\alpha}$), which is reasonably close to the observed spacing between the steps, as shown in Fig. 2a. The lattice mismatch would have been mostly accommodated by the interface steps.

The step structures of the interface, with orientation relationships ranging from NW to Kurdjumov-Sachs (KS) between two phases having face centred cubic (f.c.c.) and body centred cubic (b.c.c.) crystal structures and lattice parameter ratios, $a_{\text{f.c.c.}}/a_{\text{b.c.c.}}$, ranging from 1.25 to 1.30, have been studied theoretically and experimentally by Rigsbee and Aaronson [9, 10]. Although, the ratio of α to γ′ lattice parameters is 1.15, in the present investigation, an interface step structure with an NW orientation relationship is still formed.

3.3. Microdomain structure in the γ phase after ageing

The SAED pattern of the γ phase, after ageing at 850 °C, is similar to that of the as-solidified state, containing 90° rotational domains of $Ni_2(Mo, Al, V)$ and $Ni_3(Mo, Al, V)$ with Pt_2Mo and DO_{22} structure, respectively [11]. The only difference in the SAED pattern between the two states is that the intensity of superlattice diffraction spots of the latter is weaker than that of the former. Fig. 3 is an HREM image of the γ phase as-aged at 850 °C for 2000 h, showing fine dispersed microdomains of $Ni_2(Mo, Al, V)$ and $Ni_3(Mo, Al, V)$, of a few nanometres in size, as indicated by points "a" and "b".

Fig. 4a is an SAED pattern of the γ phase in the specimen aged at 650 °C, showing the presence of the 90° rotational domains of $Ni_2(Mo, Al, V)$ and $Ni_3(Mo, Al, V)$, and rotational domains of $Ni_4(Mo, Al, V)$ with D1a type structure. An HREM image, containing the microdomains of $Ni_2(Mo, Al, V)$, $Ni_3(Mo, Al, V)$, and $Ni_4(Mo, Al, V)$, as indicated by points "2", "3" and "4", is shown in Fig. 4b. The antiphase boundary and 90° rotational domain boundary in $Ni_3(Mo, Al, V)$ are indicated by "A" and "B", respectively.

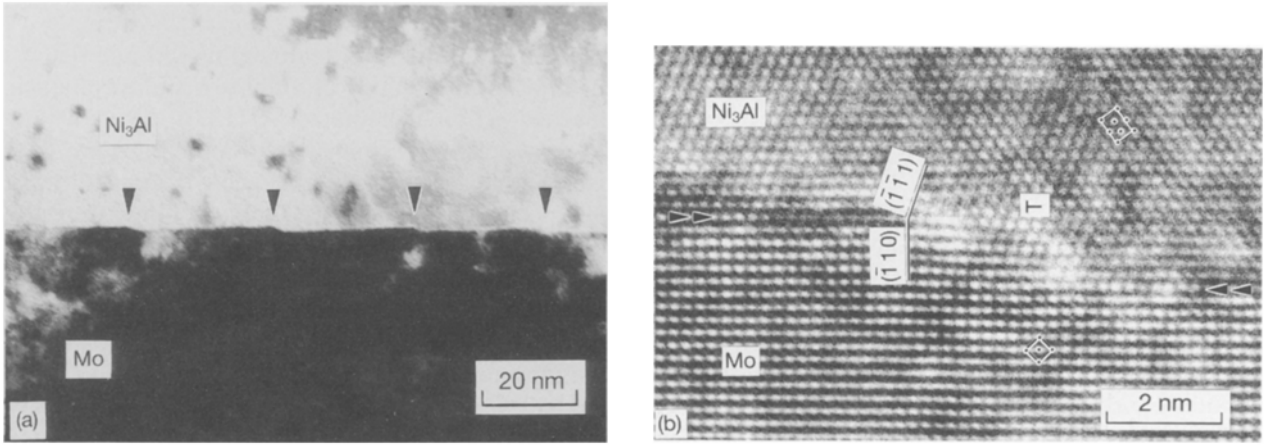

Figure 2 (a) Micrograph of α/γ′ interface with NW orientation relationship, showing regularly arranged steps with spacings ranging from 30 to 35 nm, and (b) HREM image of α/γ′ interface step viewed along $[0\,0\,1]_{\alpha}\|[1\,\bar{1}\,0]_{\gamma'}$. An extra $(1\,1\,1)_{\gamma'}$ atomic plane at the interface is indicated by the symbol "⊢".

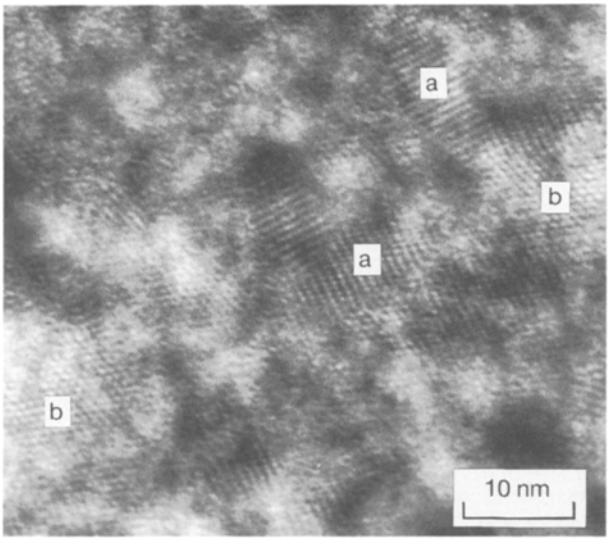

Figure 3 HREM image of the γ phase after ageing at 850 °C for 2000 h, showing the dispersed microdomains of $Ni_2(Mo, Al, V)$ and $Ni_3(Mo, Al, V)$ in the γ phase as indicated by "a" and "b".

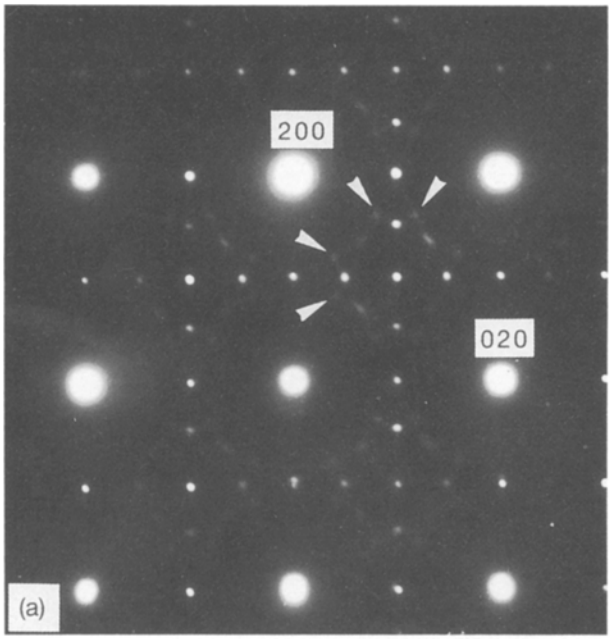

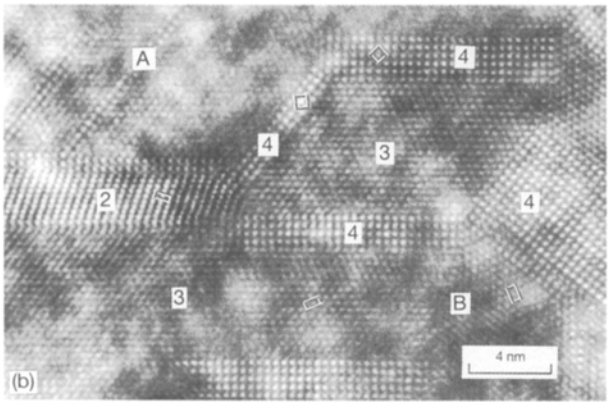

Figure 4 (a) SAED pattern of the γ phase in the specimen aged at 650 °C, showing the appearance of superlattice $Ni_4(Mo, Al, V)$ spots as indicated by arrows, and (b) on HREM image of the γ phase, showing $Ni_2(Mo, Al, V)$, $Ni_3(Mo, Al, V)$ and $Ni_4(Mo, Al, V)$ rotational microdomains, as indicated by "2", "3" and "4". The antiphase boundary and the 90° rotational domain boundary are indicated by "A" and "B", respectively.

A structural model for the formation of Ni_2Mo and Ni_4Mo in the Ni_3Mo matrix has been discussed by Tendeloo *et al.* [12]. They suggest that Ni_2Mo and Ni_4Mo may be formed from Ni_3Mo by the periodic insertion of non-conservative antiphase boundaries (APB) in the $\{1\,1\,0\}_{Ni_3Mo}$ planes. The non-conservative APBs in the $\{1\,1\,0\}_{Ni_3Mo}$ planes may be created by introducing or by extruding an Ni plane. By repeating this operation periodically in Ni_3Mo structures, Ni_2Mo and Ni_4Mo structures may be generated.

The metastable Pt_2Mo and DO_{22} type structures in this eutectic alloy are stable after prolonged ageing treatment, although the domain size decreases. The solution of Al and V in the γ phase may be causing a stability effect on the metastable Pt_2Mo and DO_{22} type structures.

The differences in the microstructure of γ phases in specimens aged at 850 and 650 °C can be attributed to the different mechanism of phase transformation, as discussed by Martin and Williams in the Ni–Mo–Al alloy system [13]. They demonstrated that various long range ordered structures, i.e. D1a, DO_{22} and Pt_2Mo prototype structures, are formed at 600, 700 and 800 °C, with a spinodal ordering transformation mechanism at temperatures lower than 700 °C, and a homogeneous nucleation mechanism at 800 °C.

3.4. Precipitation of orthorhombic Ni_3Mo and γ′–Ni_3Al in α fibres during ageing treatment

Cellular orthorhombic Ni_3Mo precipitates were found in α fibres after ageing at both 850 and 650 °C. A micrograph showing the production of precipitates along the growth direction is presented in Fig. 5. The long axes of the cellular precipitates are along $\langle 1\,1\,0\rangle_{\alpha'}$ and $-\langle 1\,1\,0\rangle_{\alpha}$, and the precipitates are tens of nanometres in size. Fig. 6 is an HREM image of the orthorhombic Ni_3Mo precipitated in the α fibre, viewed along $[0\,0\,1]_{\alpha}\|[1\,0\,2]_{Ni_3Mo}$, showing the orientation relationship between Ni_3Mo and the α fibre as follows

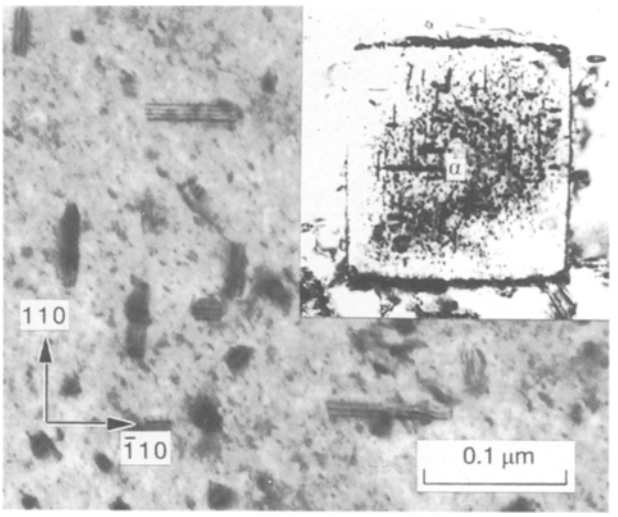

Figure 5 Micrograph of the α fibre containing cellular precipitates viewed along the growth direction. The long axes of the precipitates are along $\langle 1\,1\,0\rangle_{\alpha}$.

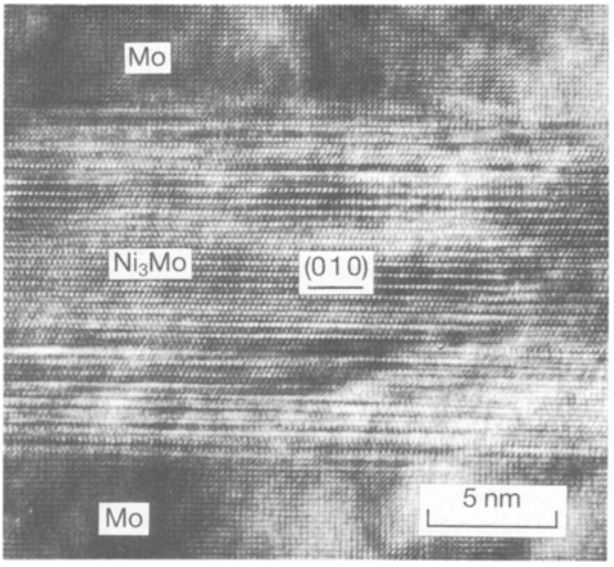

Figure 6 HREM image of orthorhombic Ni_3Mo precipitated in the α fibre viewed along $[0\,0\,1]_\alpha \| [1\,0\,2]_{Ni_3Mo}$.

$$[1\,0\,2]_{Ni_3Mo} \| [0\,0\,1]_\alpha$$

$$(0\,1\,0)_{Ni_3Mo} \| (1\,1\,0)_\alpha$$

Occasionally, a γ′–Ni_3Al precipitate was found to coexist with the Ni_3Mo precipitate inside the α fibres. Fig. 7 is an HREM image of a precipitate inside the α fibre, showing the lamellar twin structure of Ni_3Al, as indicated by "t_1" and "t_2", coexisting with Ni_3Mo. The orientation relationship between Ni_3Al and Ni_3Mo is $[1\,\bar{1}\,0]_{\gamma'} \| [1\,0\,2]_{Ni_3Mo}$ and $(1\,1\,1)_{\gamma'} \| (0\,1\,0)_{Ni_3Mo}$.

The close packed planes in Ni_3Mo and Ni_3Al, parallel to $(1\,1\,0)_\alpha$ plane, are $(0\,1\,0)_{Ni_3Mo}$ and $(1\,1\,1)_{\gamma'}$, respectively. Since the lattice mismatch at $(1\,1\,1)_{\gamma'} \| (0\,1\,1)_{Ni_3Mo}$ interface is very small (about 0.5%), γ′–Ni_3Al and orthorhombic Ni_3Mo phases can be expected to coexist in a precipitate inside the α fibres, via the coherent interface of $(1\,1\,1)_{\gamma'} \| (0\,1\,0)_{Ni_3Mo}$.

In addition, because of the structural similarity of the close packed atomic planes in Ni_3Al and Ni_3Mo, stacking faults and long period structure can be expected to form locally. Evidence for the formation of stacking faults in Ni_3Mo is given in Figs 6 and 7.

Fig. 8a, b is a composite electron diffraction pattern and schematic drawing of the diffraction pattern of Ni_3Mo, Ni_3Al and the α fibre, respectively. The extra diffraction spots, indicated by "X", correspond to the double diffraction.

Fig. 9 is an EDX spectroscopy of α fibres in specimens as-solidified state, showing the solid solution of Ni, Al and a small amount of V elements in the α fibres. Therefore, the precipitation of orthorhombic Ni_3Mo and γ′–Ni_3Al in the α fibres can contribute to the solid solution of Ni and Al in the α fibres.

Sriramamuty *et al.* [14] have reported that some fine precipitates in the α fibres were present in the specimen as-solidified state. However, the nature of these precipitates was not identified, since no diffraction effect was observed. Pearson and Lemkey have suggested that these precipitates may be carbides [15]. In the present work, these fine precipitates in the α fibres

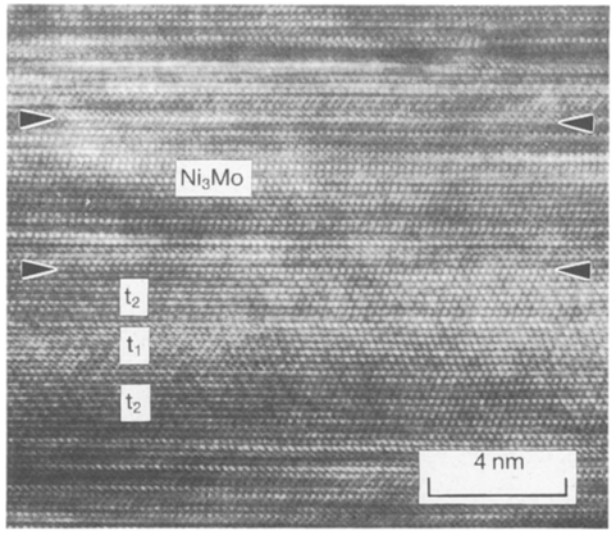

Figure 7 HREM image of the lamellar twin structure of γ′–Ni_3Al, indicated by "t_1" and "t_2", coexisting with Ni_3Mo precipitate inside the α fibre viewed along $[0\,0\,1]_\alpha \| [1\,0\,2]_{Ni_3Mo}$.

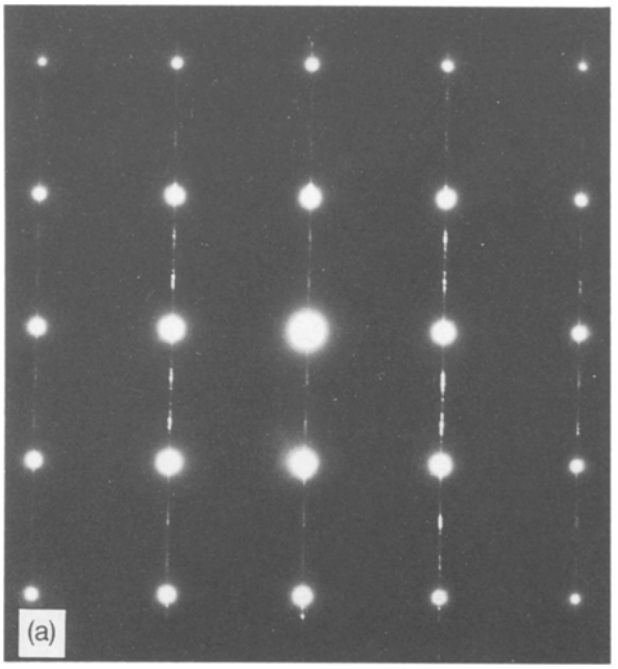

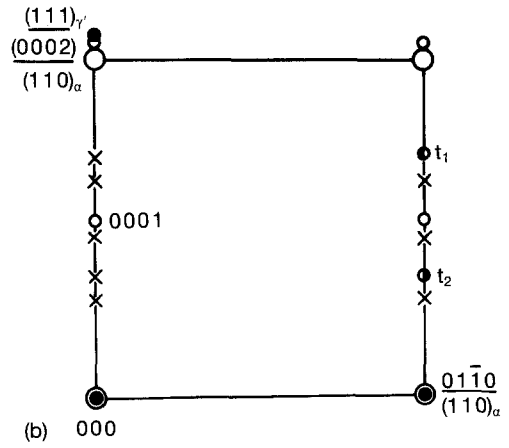

Figure 8 (a) Composite electron diffraction pattern of Ni_3Al, Ni_3Mo and the α fibre, and (b) schematic drawing of indexed diffraction patterns of Fig. 8a: (X) double diffraction spots; (○) α–Mo; (o) Ni_3Mo h.c.p. base; (◐) Ni_3Al twin 1, t_1; (◑) Ni_3Al twin 2, t_2.

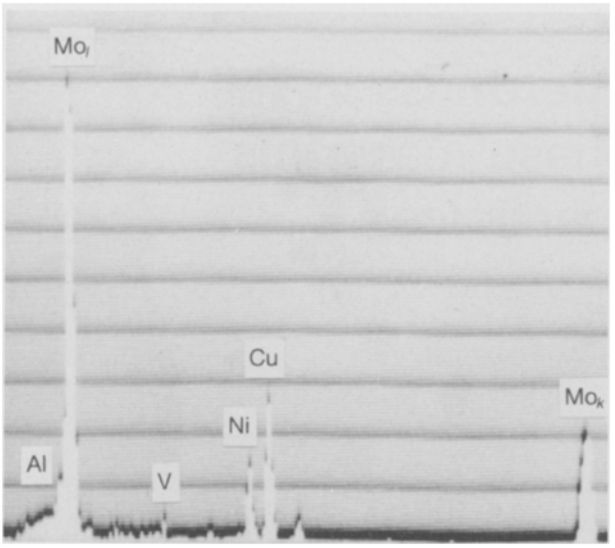

Figure 9 EDX spectroscopy showing solid solution of Ni, Al and small amounts of V elements in the α fibres.

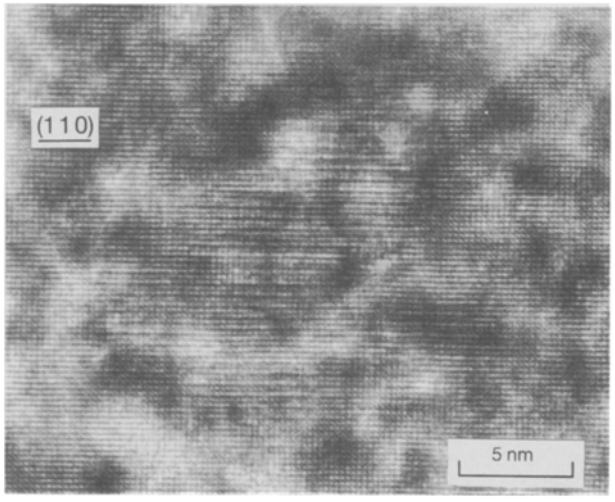

Figure 10 HREM image of the α fibre viewed along $[0\,0\,1]_{\alpha}$. The modulated fringes along $(1\,1\,0)_{\alpha}$ correspond to the initial stage of precipitation in the α fibre.

can also be observed in the as-solidified specimen. Fig. 10 is an HREM image of the α fibre observed along $[0\,0\,1]_{\alpha}$, showing the modulation fringes on the $(1\,1\,0)_{\alpha}$ planes. Since these precipitates are in an initial stage of precipitation, no geometrical shaped precipitates are identified, only the localized modulation fringes; which may be caused by the segregation of Ni and Al, can be seen.

How the fine precipitates and the growth of the precipitates during long term ageing treatment effect the mechanical properties of the material in high temperature will be explained in a further work.

4. Conclusions

1. After long time ageing treatment at 850 and 650 °C, the morphology of the α fibres is relatively stable, with typical rectangular cross-section.

2. The majority of the α fibres still display the Bain orientation relationship with the γ′/γ matrix in all of the aged specimens. In a few cases, the so-called NW orientation relationship is found in the specimen aged at 850 °C for 2000 h. The α/γ′ interface with NW orientation relationship shows step structure.

3. The 90° rotational domains of $Ni_3(Mo, Al, V)$ and $Ni_2(Mo, Al, V)$ in the γ phase change to dispersed microdomains on a nanometer scale, after ageing at 850 °C. Besides $Ni_3(Mo, Al, V)$ and $Ni_2(Mo, Al, V)$, however, an $Ni_4(Mo, Al, V)$ phase is also formed in the γ phase after ageing at 650 °C.

4. An orthorhombic Ni_3Mo phase, with a size of tens of nanometres, was found to precipitate in α fibres after ageing at both 850 and 650 °C. The orientation relationship between the precipitated Ni_3Mo and the α fibre is $[1\,0\,2]_{Ni_3Mo} \| [0\,0\,1]_{\alpha}$ and $(0\,1\,0)_{Ni_3Mo} \| (1\,1\,0)_{\alpha}$.

5. Occasionally, an γ′–Ni_3Al phase with lamellar twin structure can be found to coexist with an Ni_3Mo precipitate inside the α fibres, and displayed the following orientation relationship, $[1\,\bar{1}\,0]_{\gamma'} \| [1\,0\,2]_{Ni_3Mo}$ and $(1\,1\,1)_{\gamma'} \| (0\,1\,0)_{Ni_3Mo}$.

6. EDX analysis showed that the precipitation of Ni_3Mo and Ni_3Al is due to the solid solution of Ni and Al in α fibres.

Acknowledgements

Project supported by National Nature Science Foundation of China (NSFC) and National Advanced Materials Committee of China (NAMCC) on Grant No. 59291000.

References

1. D. D. PEARSON, B. H. KEAR and F. D. LEMKEY, in "International Conference on Creep and Fracture of Engineering Materials and Structures, University College, Swansea, 1981", edited by B. Wilshire and D. R. J. Owen (Pine Ridge Press, 1981) p. 213.
2. R. E. ANDERSEN, A. R. COX, T. D. TILLMAN and E. C. VAN REUTH, in "Proceedings of the Second International Conference on Rapid Solidification Processing, Baton Rouge, LA, 1980", edited by R. Mehrabian, B. H. Kear and M. Cohen (Claitor's Publishing Division, Baton Rouge, LA, 1980) p. 416.
3. F. H. HARF, NASA TM 81688 (1981).
4. M. J. KAUFMAN, J. A. EADES, M. H. LORETTO and H. L. FRASER, *Met. Trans.* **14A** (1983) 1561.
5. D. B. SNOW, E. M. BREINAN and B. H. KEAR, in "Superalloys", edited by J. K. Tien, S. T. Wlodek, H. Morrow, III, M. Gell and G. E. Maurer (American Society for Metals, Metals Park, OH, 1980) p. 189.
6. J. M. TARTAGLIA and N. S. STOLOFF, *Met. Trans.* **12A** (1981) 1119.
7. K. WAKASHIMA, K. HIGUCHI, T. SUZUKI and S. UMEKAWA, *Acta Metall.* **31** (1983) 1937.
8. D. B. MIRACLE, K. A. LARK, V. SRINIVASAN and H. A. LIPSITT, *Met. Trans.* **15A** (1984) 481.
9. J. M. RIGSBEE and H. I. AARONSON, *Acta Metall.* **27** (1979) 351.
10. *Idem, ibid.* **27** (1979) 365.
11. J. Y. DAI, D. X. LI, H. Q. YE, Z. X. JIN and J. H. ZHANG, *J. Mater. Sci.* **29** (1994).
12. G. VAN TENDELOO, R. DE RIDDER and S. AMELINCKX, *Phys. Status Solidi* **27A** (1975) 457.
13. P. L. MARTIN and J. C. WILLIAMS, *Acta Metall.* **32** (1984) 1681.
14. A. M. SRIRAMAMUTY, D. BANERJEE and S. N. TEWARI, *Acta Metall.* **30** (1982) 1231.
15. D. D. PEARSON and F. D. LEMKEY, in "Proceedings of the International Conference on Solidification", (Metals Society, 1979) p. 526.

Received 11 August 1993
and accepted 16 May 1994